Two-magnon Raman scattering in $KNiF_3$. A comparison of experiment with Monte Carlo calculations in the ordered and disordered regions

1997 J. Phys.: Condens. Matter 9 4979

(http://iopscience.iop.org/0953-8984/9/23/021)

J. Phys.: Condens. Matter **9** (1997) 4979–4986. Printed in the UK PII: S0953-8984(97)76169-1

Two-magnon Raman scattering in $KNiF_3$. A comparison of experiment with Monte Carlo calculations in the ordered and disordered regions

P Schilbe†, M Ramsteiner† and K H Rieder‡

† Paul-Drude-Institut für Festkörperelektronik, Hausvogteiplatz 5-7, 10177 Berlin, Germany
‡ Institut für Experimentalphysik, Freie Universität Berlin, Arnimallee 14, 14195 Berlin, Germany

Received 10 July 1996, in final form 3 December 1996

Abstract. Using Raman scattering we have investigated the behaviour of two-magnon excitations in $KNiF_3$ in dependence on the temperature especially at and above the Néel temperature (T_N). The shift of the two-magnon peak position to lower energies with increasing temperature slows down above T_N. The experimental data are compared with a simulation of the excitation process in a simple cubic Ising model, which gives a good qualitative and even quantitative description of the excitation process at and above T_N.

1. Introduction

It is well known that for antiferromagnets two-magnon excitations in Raman scattering persist even above the Néel temperature [1, 2]. Two-magnon Raman scattering has been observed for many antiferromagnets of various crystal structures [1, 2]. Most of these investigations were made in the early seventies. In the last few years magnon excitations in solids have gained renewed interest due to the antiferromagnetic ordering of the insulating parent compounds of many high-T_c superconductors [3, 4].

The excitation of magnons in simple transition-metal halides, such as $KNiF_3$, $KCoF_3$ and MnF_2, up to the Néel temperature is now well understood [1, 2]. The theoretical description of the scattering process is in good agreement with the experimental observations [1, 2]. The line shape and the dependence of the two-magnon peak on the temperature are well described by theoretical calculations. At low temperatures Green's function calculations with second-order Hartree–Fock renormalization of the magnon energies give a very good agreement between theory and experiment [5]. At and above the critical temperature the presence of many thermally excited magnons, which lead to the breakdown of the magnetic order, and the strong magnon-magnon interaction make theoretical calculations difficult [2]. Consequently, the theoretical calculations considered so far give only a crude description of the two-magnon Raman scattering data at and above the Néel temperature. Only a modified Markoffian approximation for the continued-fraction representation of the shape function gives better results at T_N and $T = \infty$ [6]. At intermediate temperatures the unknown temperature dependence of the input parameters of the continued-fraction representation makes a reasonable estimate of the peak position difficult.

For a comparison of theoretical predictions with experimental two-magnon Raman scattering data, $KNiF_3$ has several advantages: the exchange interaction is practically

0953-8984/97/234979+08$19.50

restricted to nearest neighbours, the magnetic anisotropy is small, there are no first-order Raman active phonons and no structural phase transition is known. The interaction is well described by the Heisenberg model and the angular momentum ($S = 1$) of the Ni ions is solely the spin of the valence electrons [7]. The value of the exchange constant is $J = 70.9$ cm^{-1}. $KNiF_3$ belongs to the space group O_h^1 with a cubic perovskite structure. In the magnetically ordered temperature region a small tetragonal distortion due to magnetostrictive effects is observed [8], which is absent from the disordered regime.

Two-magnon Raman scattering for $KNiF_3$ was observed up to 300 K [9, 10]. Below T_N the agreement between theory and experiment is, as mentioned above, very good [5, 6]. However, around the Néel temperature $T_N = 246$ K [11] the experimental values are less accurate due the small intensity and the large width of the two-magnon peaks in this temperature region.

We present very accurate Raman data for the two-magnon position and width of $KNiF_3$, especially at and above T_N. The experimental data are compared to Monte Carlo calculations, which are able to explain the observed two-magnon behaviour even above T_N.

2. Raman scattering in $KNiF_3$

The experiments were performed on a transparent single-crystal sample of $KNiF_3$ of size $5\times5\times3$ mm^3 with bright green colour. All spectra shown here were taken in a backscattering geometry $[z(x, y)\bar{z}]$ with the x, y, z directions parallel to the $\langle100\rangle$ directions and were excited by 0.5 W of the 514.5 nm laser line of an argon ion laser. The spectral resolution was 3 cm^{-1}. The dominant feature of the Raman spectrum of $KNiF_3$ at 50 K shown in figure 1 is the two-magnon peak at about 800 cm^{-1}, which shifts to lower energies and decreases in peak height at higher temperatures (figure 2). The two-magnon scattering will be discussed below. Below 800 cm^{-1} small peaks appear in the spectra. The observed peak positions do not coincide with the phonon energies observed in infrared (IR) spectroscopy [12, 13]. Some of them have even higher energies than the phonon modes observed in

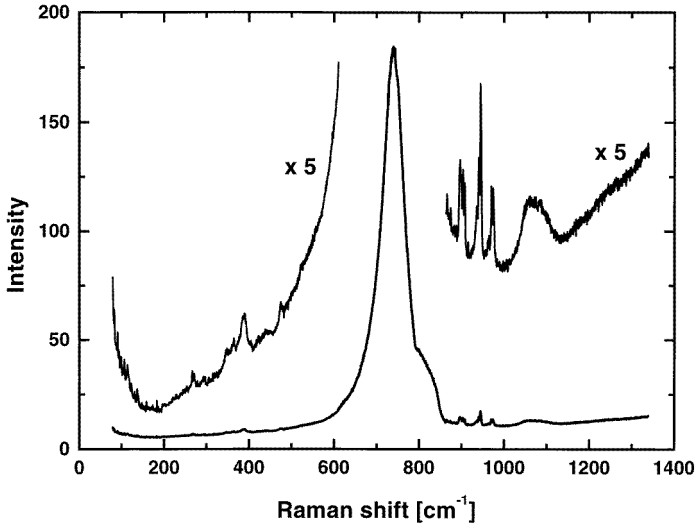

Figure 1. The depolarized low-temperature (50 K) Raman spectrum of $KNiF_3$ excited at 5145 Å.

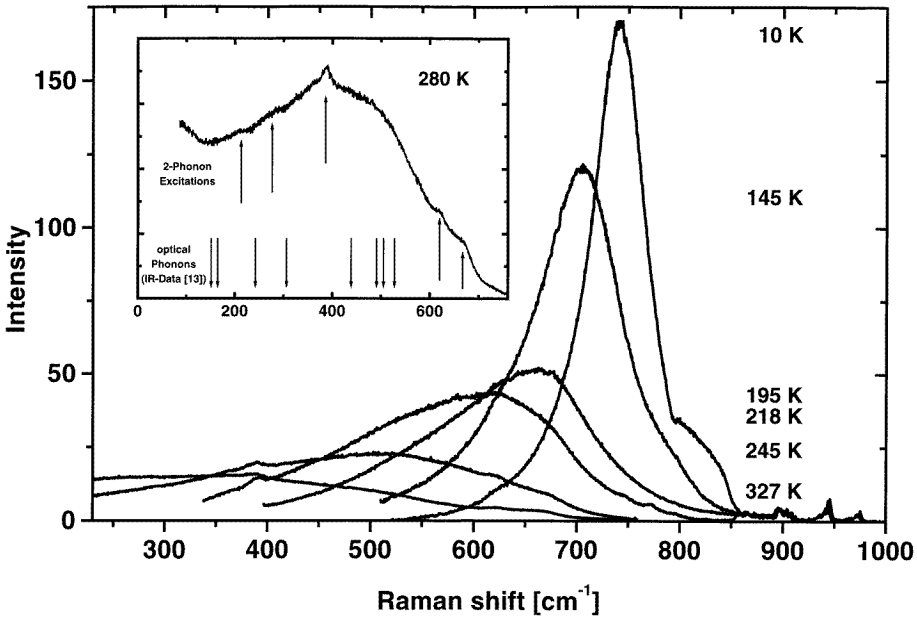

Figure 2. Two-magnon Raman spectra of $KNiF_3$. The inset shows, for a room-temperature spectrum, the location of the two phonon modes (marked with up arrows) and the position of the optical phonons observed in IR spectroscopy [12] (down arrows).

IR spectroscopy. First-order Raman scattering by optical phonons due to the deformation-potential mechanism is symmetry forbidden for $KNiF_3$ [9]. Other scattering mechanisms with different symmetry selection rules takes place. For example, in $KCoF_3$ [14], where the angular momentum of the Co ion is partly due to the orbital angular momentum, normally Raman-forbidden single-phonon modes are observable. However, in contrast to $KCoF_3$, $KNiF_3$ is a pure spin system. The small tetragonal distortion in the ordered region is not able to produce first-order allowed phonon modes since a tetragonal distortion does lead to Raman-allowed first-order phonon scattering. The energies of the small peaks below 800 cm^{-1} are compatible with the expected energies of two-phonon modes. Therefore we attribute these peaks to second-order phonon scattering. An assignment of these peaks to the various combinations of optical and acoustical phonons is not possible because to our knowledge no phonon dispersion data are available for $KNiF_3$. The relatively broad peak at 1060 cm^{-1} is also a two-phonon mode (figure 3) [15]. The energy of this peak agrees with twice the energy of the highest optical phonon with $\nu_{LO} = 530$ cm^{-1} observed in IR spectroscopy [12, 13]. This phonon mode is mainly a bending vibration of the F–Ni–F bond. Tomono *et al* [13] observed a down-shift of 15 cm^{-1} for the corresponding TO mode with increasing temperature from 0 to 300 K. In the inset of figure 3 the peak position of the two-phonon peak is shown as a function of temperature. The down-shift of 18 cm^{-1} is only slightly larger than the shift of the single TO phonon peak in IR spectra. The other two-phonon peaks show, within the experimental error, no energy shift with temperature, which is in accordance with the observation of Tomono *et al* [13]. The influence of the long-range magnetic order on the energy shift of the highest two-phonon mode at 1060 cm^{-1} is clearly seen by the abrupt change in the slope of the shift exactly at T_N. This downward shift originates from a contribution of the superexchange interaction to the Ni–F–Ni bond

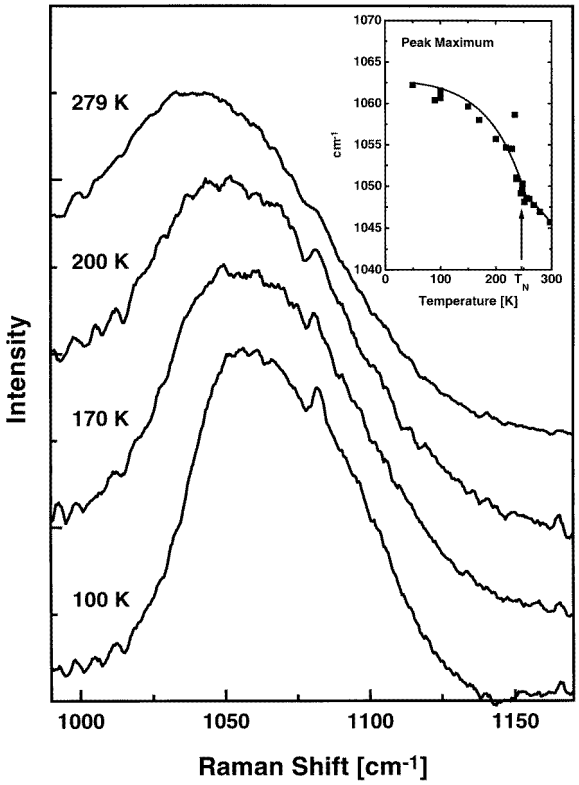

Figure 3. Two-phonon excitation in $KNiF_3$. The shift of the peak maximum is depicted in the inset. The solid line is a guide to the eye. The slope of the peak shift shows a sudden change at the Néel temperature.

[13]. This behaviour has also been found in other magnetic compounds, e.g. on $YCrO_3$ or $GdCrO_3$ [16].

We were not able to observe a four-magnon peak, which is in conflict with the measurements of Dietz *et al* [15]. Only a very weak feature is seen at 1270 cm^{-1} in some spectra, the position where Dietz *et al* observed a clearly visible peak, which they assigned to a four-magnon excitation.

The origin of the small sharp peaks at 900 cm^{-1} (figure 1) is unclear. They show a very small peak width and seem to be arranged in four groups of three peaks each. Therefore it seems to be unlikely that they are two-phonon modes. They cannot be attributed to any known electronic transition in $KNiF_3$ [17, 18]. A small downward shift with increasing temperature is observed for these peaks. It appears to be possible that they are due to contaminations of the crystal.

3. Monte Carlo simulations for two-magnon excitations

The density of states of magnons is sharply peaked at the Brillouin zone boundary. Therefore it is possible to simulate the excitation of magnons which are observed in Raman scattering within an Ising model [2]. The Ising model appropriate for $KNiF_3$ consists of a simple

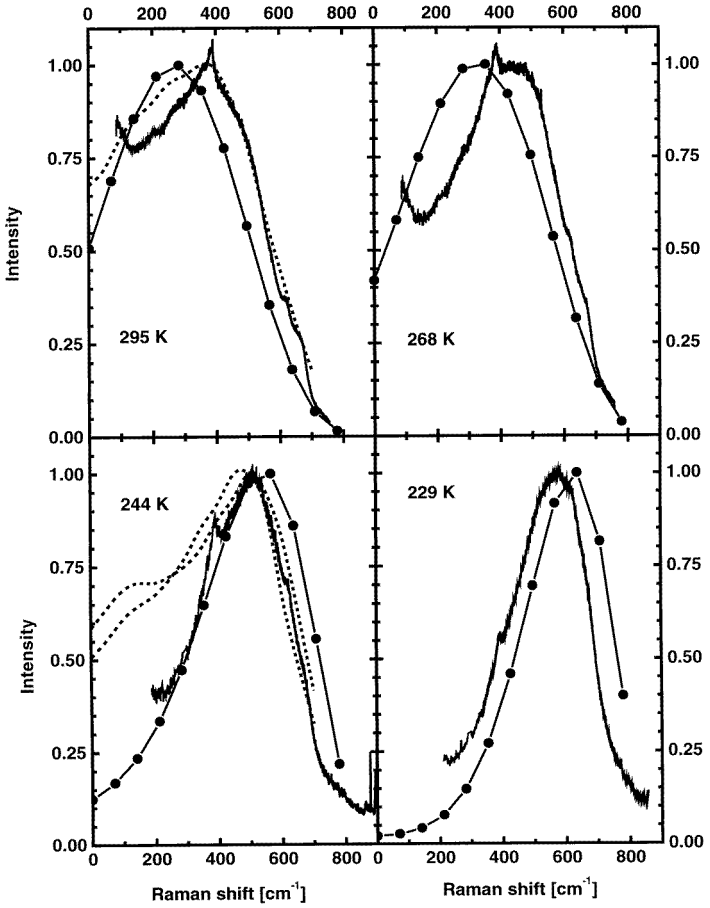

Figure 4. A comparison of the experimental two-magnon spectra (solid lines), theoretical results from a continued-fraction approach for the Raman cross section from [6] (dashed lines), and the MC data for the spin-1 Ising model (circles connected with straight lines) for different temperatures. The shapes of the experimental peaks and the MC calculations are very similar. The increase in the intensity of the experimental spectra at very small frequencies (< 200 cm^{-1}) originates from the Rayleigh line. The small peak at 400 cm^{-1} is a two-phonon mode of $KNiF_3$.

cubic $S = 1$ spin lattice with an antiferromagnetic coupling between nearest neighbours. Starting from a completely ordered spin–lattice the excitation of two magnons is simulated by the change of two spins on neighbouring sites from $S = +1/S = -1$ to $S = 0$; the other spins remain unchanged. The necessary energy ΔE depends on the coupling constant J, the spin S and the coordination number z (here $z = 6$):

$$\Delta E = 2(z-1)JS^2 + JS^2. \tag{1}$$

The resulting value agrees reasonably with the experimental date [1, 2] for many antiferromagnets, and is in fact often used to estimate the exchange constant J. The interaction of magnons in the Heisenberg model results in a smaller energy being necessary to excite two magnons simultaneously in Raman scattering than two magnons with the same k-vector separately. In the Ising model this is also incorporated simply by the fact that the two spins are located at neighbouring sites. For higher temperatures in the Heisenberg

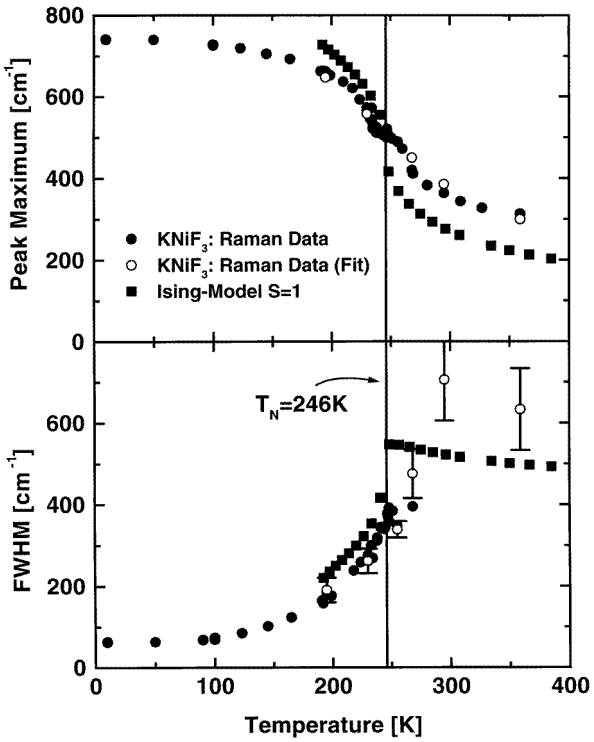

Figure 5. A comparison of the peak position and full width at half maximum (FWHM) of the experimental two-magnon spectra for $KNiF_3$ (circles) with the MC simulations for the spin-1 Ising model (squares). The open circles are the maximum and the FWHM of a fit to the experimental data. The closed circles are the absolute maximum and the FWHM including the two-phonon losses. Above T_N the determination of the FWHM is difficult because the peak leaks into the anti-Stokes regime and the tail of the laser beam has to be subtracted.

model the thermally excited magnons lead to a further down-shift of the two-magnon peak and to an increase of the peak width due to damping of the magnons. These two properties of the two-magnon spectra are also incorporated in the Ising model due to the increasing disorder of the neighbouring sites. At higher temperatures more neighbouring spins are excited and the energy necessary to change to neighbouring spins is reduced. The width of the two-magnon peak at elevated temperatures is reflected by the larger number of states of the surrounding spins that are occupied. Thus a Monte Carlo (MC) calculation for a simple cubic $S = 1$ Ising model, in which the energy necessary to excite two neighbouring spins is calculated in dependence on the temperature, should give an estimate of the peak position and width of two-magnon excitations in Raman spectroscopy even at temperatures higher than the Néel temperature. Moreover this approach takes into account that at temperatures near and above T_N the magnons are strongly damped and there is no long-range order present, so the picture of a local excitation should give better results than the concept of extended spin waves. The only input parameters are the exchange constant and the Néel temperature. This is an advantage over the continued-fraction representation where the time dependence of the Laplace transformation of the continued-fraction representation of the shape function has to be chosen to be reasonable [6].

The MC calculations were performed with the single-spin-flip Metropolis algorithm [19]. With this algorithm it is easier to incorporate next-nearest-neighbour interaction and anisotropies than in a cluster algorithm. The model consists of a cubic spin-1 Ising model with periodic boundary conditions. At the beginning up to 10^4 MC steps have been discarded to reach equilibrium (in one MC step each spin in the lattice is tested once whether it is changed or not). After this for every third MC step the magnetization m of the two sublattices, the square m^2 and m^4 were evaluated and for each pair of antiparallel spins in the lattice the energy was calculated to excite these two spins to $S = 0$.

4. A comparison of the experiment and the simple model for two-magnon excitations

In figure 4 the results of the MC calculations are compared with the experimental data for the two-magnon scattering in $KNiF_3$. For the Ising model the exchange constant was chosen to be $J = 70.9$ cm^{-1}, which is the experimental value [9]. The absolute temperatures for the Ising model were calculated from the reduced temperatures $1 - T/T_N$ with the critical temperature of $T_N = 246$ K for $KNiF_3$. The intensities of the peaks were normalized to unity. The main features of the experimental data are well reproduced by the MC calculations: the shift of the peak maximum to lower energies and the increase of the width with increasing temperature as well as the asymmetry of the two-magnon peak with a tail to lower energies. A direct comparison of the peak position and the peak width is shown in figure 5. For the MC data an asymmetric sigmoidal function was fitted to the data to give a reliable measure of the peak position and width. The determination of the peak position and peak width of the experimental two-magnon peaks is obscured by the presence of the two-phonon peaks just in the energy range where the two-magnon peak lies at higher temperatures. To determine the width and the peak position more accurately the experimental data were fitted for some temperatures by an asymmetric sigmoidal function for the two-magnon peak and Gauss functions for the two-phonon peaks. The tail of the Rayleigh line at low energies was also subtracted form the two-magnon peak. The peak position (figure 5, top) decreases monotonically with increasing temperature. Above T_N the slope of the curve decreases. Due to the large width of the peak this behaviour of the two-magnon peak had not yet been observed for $KNiF_3$. It occurs also for other antiferromagnets (e.g. $RbCoF_3$, $RbMnF_3$, NiF_2 [20, 21]). The decrease of the slope of the experimental curve at T_N is due to a two-phonon peak, which overlaps with the two-magnon peak at T_N. The Ising data show a very similar behaviour. The theoretical curve crosses the experimental data exactly at T_N. Below T_N the peak for the Ising model moves faster to higher energies with decreasing temperatures than the experimental peak. This deviation is expected since in the ordered region the excitation energy of two neighbouring sites should be higher than the energy of the extended spin wave. The decrease of the slope in the model calculations above T_N shows that the corresponding behaviour in the antiferromagnets results from a slower decrease of the nearest-neighbour correlation function with higher temperatures. The width of the peak in the Ising model shows a surprising behaviour at first glance. It increases up to T_N and remains nearly constant at higher temperatures with a slight tendency to smaller values at very high temperatures. Below T_N the FWHMs of the experimental data agree very well with the Ising model. Due to the difficulties in the determination of the experimental peak widths above T_N the corresponding data contain a large uncertainty. Nevertheless the peak width seems to remain constant within the error bars or at least increases much more slowly. This can be also seen by direct comparison of the experimental data at different temperatures (figure 4). The shapes of the peaks at temperatures near and above T_N are very similar. The leakage of the two-magnon peak into the anti-Stokes regime is also observable

in the model calculation. This shows that the simple Ising model gives indeed a reliable description of the excitation process above the Néel temperature.

A comparison of the results of the continued-fraction approach for the Raman cross section [6] with the experimental data (figure 4) shows that the continued-fraction calculation reproduces the experimental data at high wavenumbers quite well but overestimates the cross section for lower energies. Hence the shape of the two-magnon peak is better reproduced by the MC data and the continued-fraction data give a better description of the high-energy part of the peak.

5. Conclusion

We have measured the peak position and the peak width of the two-magnon excitation in Raman scattering for $KNiF_3$. At and above T_N we were able to determine the shape and the position of the peak very accurately. Therefore a better comparison between experimental data and theoretical calculations was possible. The slowing down of the peak position decrease above T_N had not been observable in previous investigations for $KNiF_3$. MC calculations on the simple cubic Ising model give a simple description of the excitation process. The qualitative behaviour of the two-magnon peak is well described by the Ising model. This means that the peak shift, the variation of the FWHM and the shape of the two-magnon peak are in good agreement with the model calculations. Above T_N the FWHM calculated from the Ising model remains nearly constant, as also observed experimentally. The Ising model even gives a good quantitative estimate of the position and the width of the two-magnon peak in the temperature region around the phase transition.

References

[1] Lockwood D J 1982 *Light Scattering in Solids III (Topics in Applied Physics 51)* ed M Cardona and G Güntherodt (Berlin: Springer) p 59
[2] Balucani U and Tognetti V 1976 *Riv. Nuovo Cimento* **6** 39
[3] Thomsen C 1991 *Light Scattering in High-T_c-Superconductors, Light Scattering in Solids VI (Topics in Applied Physics 68)* ed M Cardona and G Güntherodt (Berlin: Springer)
[4] Chubkov A V and Frenkel D M 1995 *Phys. Rev.* B **52** 9760
[5] Balucani U and Tognetti V 1973 *Phys. Rev.* B **8** 4247
[6] Balucani U and Tognetti V 1977 *Phys. Rev.* B **16** 271
[7] Cowley R A and Buyers W J L 1972 *Rev. Mod. Phys.* **44** 406
[8] Money D G, Paige D M, Corner W D and Turner B K 1980 *J. Magn. Magn. Mater.* **15–18** 603
[9] Chinn S R, Zeiger H J and O'Connor J R 1971 *Phys. Rev.* B **3** 1709
[10] Fleury P A, Hayes W and Guggenheim H J 1975 *J. Phys. C: Solid State Phys.* **8** 2183
[11] Ferré J, Jamet J P and Kleemann W 1982 *Solid State Commun.* **44** 485
[12] Barker A S Jr, Ditzenberger J A and Guggenheim H J 1969 *Phys. Rev.* **175** 1180
[13] Tomono Y, Takaoka T, Yajima M, Tanokura Y and Jinda N 1990 *J. Phys. Soc. Japan* **59** 579
[14] Holden T M, Buyers W J, Svensson E C, Cowley R A, Hutchings M T, Hukin D and Stenvenson R W H 1971 *J. Phys. C: Solid State Phys.* **4** 2127
[15] Dietz R E, Brinkman W F, Meixner A E and Guggenheim H J 1971 *Phys. Rev. Lett.* **27** 814
[16] Udagawa M, Kohn K, Koshizuka N, Tsushima T and Tsushima K 1975 *Solid State Commun.* **16** 779
[17] Ferguson J, Guggenheim H J and Wood D L 1964 *J. Chem. Phys.* **40** 822
[18] Abdalian A T and Moch P 1978 *J. Appl. Phys.* **49** 2189
[19] Binder K and Heerman D W 1988 *Monte Carlo Simulations in Statistical Physics* (Berlin: Springer)
[20] Fleury P A 1970 *J. Appl. Phys.* **41** 886
[21] Nouet J, Toms D J and Scott J F 1973 *Phys. Rev.* B **7** 4874